IUGG 2015
JM02p-307

Analysis of Global Climate Variability from Homogenously Reprocessed Ground-based GNSS Measurements

Furqan Ahmed(1), Addisu Hunegnaw(1), Norman Teferle(1) and Richard Bingley(2)

1) Geophysics Laboratory, University of Luxembourg, Luxembourg
2) Nottingham Geospatial Institute, University of Nottingham, United Kingdom

Contact: furqan.ahmed@uni.lu

Download this poster:

Abstract

The tropospheric delay information obtained through long-term homogenous reprocessing of Global Navigation Satellite System (GNSS) observations can be used for climate change and variability analysis on a global scale. A reprocessed global dataset of GNSS-derived zenith total delay (ZTD) and position estimates, based on the network double differencing (DD) strategy and covering 1995-2012, has been recently produced at the University of Luxembourg using the Bernese GNSS Software 5.2 (BSW5.2) and the reprocessed products from the Centre for Orbit Determination in Europe (CODE). The network of ground-based GNSS stations processed to obtain this dataset consists of over 400 globally distributed stations. The GNSS-derived ZTD has been validated by comparing it to that derived from reanalysis data from the European Centre for Medium-Range Weather Forecasts (ECMWF). After validation and quality control, the ZTD dataset obtained using the DD strategy has been used to investigate the monthly and seasonal climate variability in the tropospheric delay on various regional to global spatial scales. Precise point positioning (PPP) is a processing strategy for GNSS observations which is based on observations from a single station rather than a network of baselines and is therefore computationally more efficient than the DD strategy. However, the two processing strategies, i.e. DD and PPP, have their own strengths and weaknesses and could affect the solutions differently at different geographical locations. In order to explore the use of PPP strategy for climate monitoring, another experimental dataset covering a shorter period has been produced using the PPP strategy and compared to the DD based ZTD dataset.

Introduction

Atmospheric water vapour is the most abundant greenhouse gas and plays a significant role in weather formation, climate change and global warming. Therefore, precise knowledge of the quantity of water vapour in the atmosphere helps in the improvements of weather forecasts and climate monitoring. It is widely known that the propagation delay experienced by GNSS signals, namely the zenith total delay (ZTD), can be converted to integrated water vapour (IWV) using surface meteorological data [1]. As of today, GNSS observations from global networks are available for about the last two decades and this makes it possible to use GNSS as a climate monitoring tool by reprocessing the long-term historical observations and obtaining the IWV trends. Other than its use in climate monitoring, GNSS-derived near real-time ZTD data is assimilated into numerical weather prediction models to improve the short-term weather forecasts. Precise point positioning (PPP) and double differencing (DD) are the common strategies in use today for processing of GNSS observations. PPP solutions are based on single station observations and are mainly affected by the quality of orbit/clock products. DD solutions, on the other hand, are based on differenced observations between the stations in a network and while the dependency on the products is much smaller. DD results are somewhat affected by the distance between stations, especially of remote stations at mid-ocean islands.

In this study, the ZTD dataset obtained by the DD processing strategy has been used to study the variability in climate on different temporal scales for 7 regions ranging from High North (HN) to High South (HS) based on latitude. Furthermore, a comparison of DD and PPP ZTD estimates has been conducted in order to study the suitability of the PPP strategy for climate monitoring. The DD and PPP solutions used for this study will hereafter be denoted as DDUL and PPUL, respectively. Table 1 shows the processing characteristics of DDUL and PPUL.

Table 1: Processing characteristics of the ZTD estimation systems

Solution Type:	Precise Point Positioning	Double Differencing
Strategy:	PPP	DD
Processing Engine:	BSW5.2 [2]	BSW5.2
ZTD Output Interval:	2 hours	1 hour
Observation Window Used:	24 hours	24 hours
Processing Session Length:	24 hours	24 hours
GNSS Used:	GPS	GPS
Ionosphere	1st and 2nd order effect	1st and 2nd order effect
A-Priori ZHD Model:	VMF	VMF
Troposphere Mapping Function:	VMF1	VMF1
Orbit Product Used:	MI2	COD Repro2
Clock Product Used:	MI2	-
Antenna Models:	IGS08	IGS08
Coordinates Computed:	Yes	Yes
Elevation Cut-Off Angle:	3°	3°
Ambiguity Resolution:	No	Yes

The ground-based GNSS network used in the DDUL solution comprises of around 450 globally distributed stations (Figure 1). Figure 1 also shows the division of GNSS stations in 7 latitude-based regions coded using different colors.

The evolution of the number of processed stations with time is shown in Figure 2. The network processed in the PPUL solution is a subset of the DDUL network, which comprises of 84 globally distributed IGb08 core stations from the reference frame network of the International GNSS Service (IGS) [3].

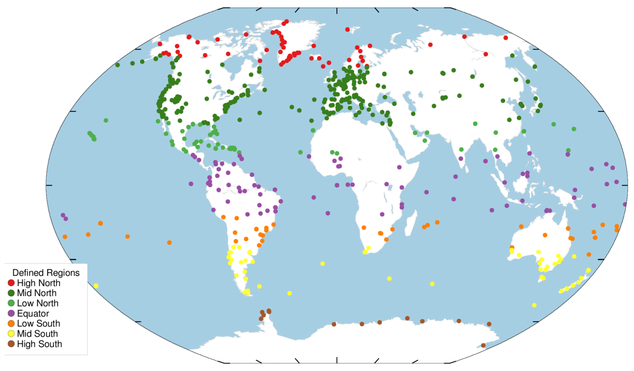

Figure 1 The network of stations processed in the DDUL solution and the region specification

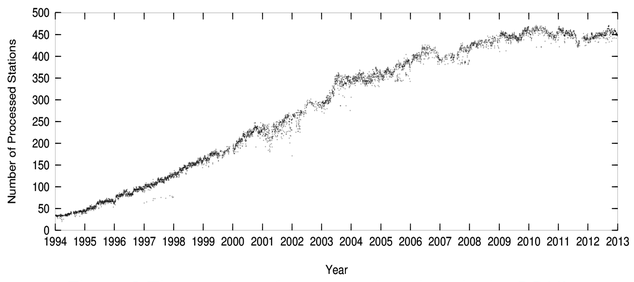

Figure 2 The number of processed stations in the DDUL solution

Validation of GNSS-Derived ZTD Estimates

Prior to their use in climate monitoring, the GNSS-derived ZTD estimates from the DDUL solution have been validated using the ZTD derived from the European Centre for Medium-range Weather Forecasts (ECMWF)'s reanalysis dataset ECMWF Reanalysis-Interim (ERA-Interim). The validation has been performed by the 5-year long GNSS and ERA-Interim ZTD time series for one randomly selected station in each of the defined regions (Table 2, Figure 3). It could be seen from Figure 3 and Table 2 that the time series of GNSS-derived ZTD and ERA-Interim ZTD follow the same pattern, however, a millimeter level bias exists between the two.

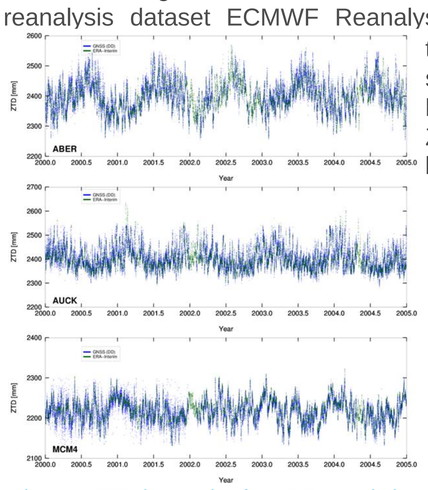

Figure 3 ZTD time series from DDUL solution (blue) and ERA-Interim (green)

Table 2: Difference between GNSS-derived ZTD and ERA-Interim ZTD

Station	Region	$Difference_{GNSS-ERA}$ [mm]	$STD_{GNSS-ERA}$ [mm]	$RMS_{GNSS-ERA}$ [mm]
ALRT	High North	-4.77	5.68	7.41
ABER	Mid North	3.63	11.28	11.85
BAHR	Low North	-7.34	15.83	17.45
ASC1	Equator	4.08	12.84	13.48
ALIC	Low South	9.51	14.52	17.36
AUCK	Mid South	3.98	12.71	13.32
MCM4	High South	-1.95	10.64	10.82

Monthly and Seasonal Variability in ZTD

In order to study the variability in the ZTD for the 7 defined regions (Figure 1) on monthly and seasonal scales, monthly and seasonal ZTD means for all the stations in each region were averaged. Four seasons were defined by combining three months i.e. December-January-February (DJF), March-April-May (MAM), June-July-August (JJA) and September-October-November (SON). Figure 4 presents the region-wise time series of monthly and seasonal means (after subtracting the values) and shows that the ZTD in the LN and LS regions has the highest variability whereas the HS region has the lowest variability. Similarly, it can be seen that the maximum value of ZTD occurs during JJA season in the northern hemisphere and in DJF season in the southern hemisphere.

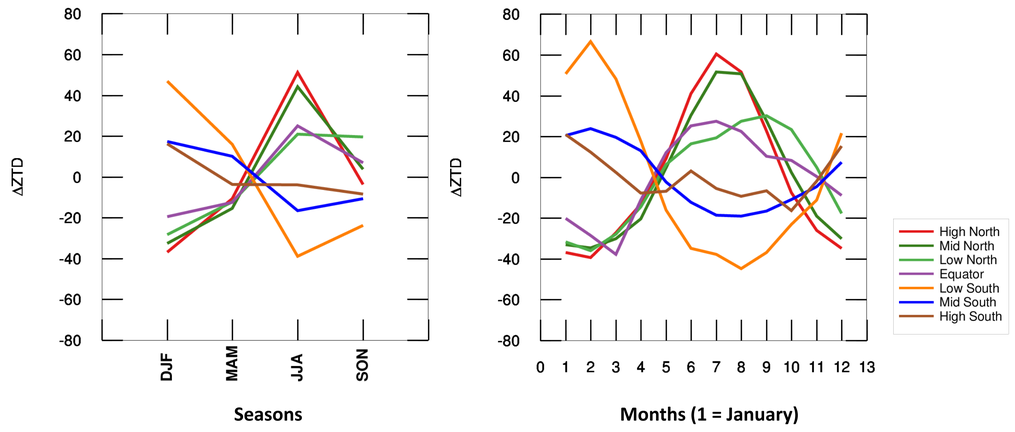

Figure 4 Seasonal (left) and monthly (right) averages of ZTD for the various regions

Comparison of Precise Point Positioning and Double Differenced ZTD Estimates

The PPP strategy is computationally more efficient than DD network solutions and requires less resources for processing large amounts of data. Therefore, it is of interest to study the suitability of the PPP strategy for climate monitoring applications. To serve this purpose, two comparisons (one using the GPT/GMF and another using the VMF1[4] mapping functions) of the ZTD estimates from DDUL (ZTD_{DD}) and PPUL (ZTD_{PPP}) solutions have been conducted for 84 selected IGb08 core stations and the year 2001. Table 3 shows the overall statistics of these comparisons and suggests that the agreement between ZTD_{PPP} and ZTD_{DD} improves with the use of VMF1.

Table 3: Difference between ZTD_{PPP} and ZTD_{DD}

Mapping Function	$Bias_{PPP-DD}$ [mm]	STD_{PPP-DD} [mm]	RMS_{PPP-DD} [mm]
GPT/GMF	-1.35	12.98	14.09
VMF1	-0.68	10.13	10.59

Figure 5 shows, for two randomly selected stations, the correlation plot between ZTD_{PPP} and ZTD_{DD} whereas Table 4 shows the correlation coefficients between ZTD_{PPP} and ZTD_{DD} for one station in each of the 7 regions. In general, the correlation is higher for ZTDs computed using VMF1 and the correlation values are more consistent for ZTDs using VMF1. Furthermore, station-specific effects seem to have a larger impact on PPP solutions when using GPT/GMF.

Table 4: Correlation between ZTD derived using PPP and DD strategies

Station	Region	Using GPT/GMF	Using VMF1
NYA1	High North	1.0000	0.9962
NANO	Mid North	0.9007	0.9972
LHAS	Low North	0.9045	0.9687
LAE1	Equator	0.8137	0.9586
ALIC	Low South	0.9693	0.9692
CHAT	Mid South	0.9286	0.9813
MCM4	High South	0.5460	0.8417

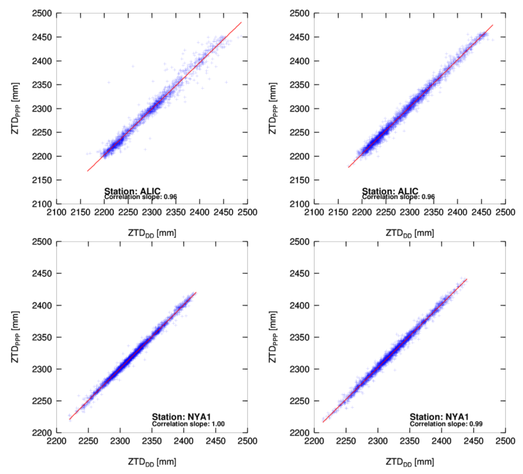

Figure 5: Correlation between ZTD_{PPP} and ZTD_{DD} using GPT/GMF (left column) and VMF1 (right column) for the stations ALIC (top row) and NYA1 (bottom row)

Figure 6 shows the latitude dependence of the RMS differences between ZTD_{PPP} and ZTD_{DD} when using GPT/GMF (left) and VMF1 (right) mapping functions. It can be seen that in both cases, the maximum of the difference occurs around the equator which can be attributed to the maximum concentration of water vapour around the equator. However, when using VMF1, the scatter of the RMS difference is smaller than that obtained by using GPT/GMF.

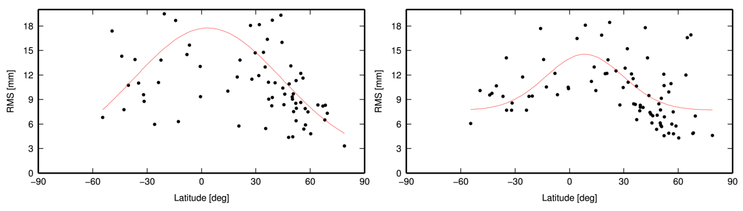

Figure 6: Latitude dependence of the RMS difference between ZTDPPP and ZTDDD obtained using GPT/GMF (left) and VMF1 (right)

Conclusions

A 19-year long global reprocessed GNSS data set based on the double differencing strategy has been used to study the variability of GNSS-derived ZTD on various temporal scales for the seven regions specified based on latitude. The GNSS-derived ZTD has been validated by comparing it to that derived from the ERA-Interim re-analysis data set for a period of five years. For the 5-year period, a millimeter-level agreement has been found between the GNSS and ERA-Interim ZTD.

Variation in ZTD on monthly and seasonal scales have been studied by computing monthly and seasonal averages for each region. It has been found that the ZTD in the Low North and Low South regions has the highest variability whereas the High South region has the lowest variability. Similarly, it can be seen that the maximum value of ZTD occurs during the JJA season in the northern hemisphere and in the DJF season in the southern hemisphere.

A comparison between the ZTD estimated from the PPP and DD processing strategies has been performed using the GPT/GMF as well as the VMF1 mapping functions. It has been found that regardless of the used mapping function, there is a millimeter level agreement and a strong correlation between ZTD_{PPP} and ZTD_{DD}. The difference between ZTD_{PPP} and ZTD_{DD} has been found to have a latitude dependence with a maximum around the equator, regardless of the used mapping function. However, the use of VMF1 has improved the agreement between ZTD_{PPP} and ZTD_{DD}.

References
[1] Bevis, M., S. Businger, Chiswell S., T. A. Herring, R. A. Anthes, C. Rocken, R. H. Ware (1994) GPS Meteorology: Mapping Zenith Wet Delays onto Precipitable Water, Journal of Applied Meteorology, 33(3), 379-386
[2] Dach R (2013) Bernese GNSS Software: New features in version 5.2, Astronomical Institute, University of Bern, Bern, Switzerland
[3] Dow, John M and Neilan, R E and Rizos, C (2009) The International GNSS Service in a changing landscape of Global Navigation Satellite Systems. Journal of Geodesy 83(3-4), 191–198
[4] Boehm J, B Werl, H Schuh (2006a) Troposphere mapping functions for GPS and very long baseline interferometry from European Centre for Medium-Range Weather Forecasts operational analysis data. Journal of Geophysical Research 111 B02406

Acknowledgements
This project is funded by the *Fonds National de la Recherche, Luxembourg (Reference No. 1090247)*. The data reprocessing campaign was carried on the University of Luxembourg's High Performance Computing (HPC) cluster under the "New Geodetic Infrastructure and Re-processed GPS Solutions for Sea Level, Climate and Geodynamics (GSCG)" project funded by the University of Luxembourg. We also thank the TIGA, BIGF, CODE, EUREF, and IGS communities for GNSS data and products.

Presented at: *26th General Assembly of the IUGG, Prague, Czech Republic, June 22-July 2, 2015*